Protein Expression and Purification 75 (2011) 127–132

Contents lists available at ScienceDirect

Protein Expression and Purification

journal homepage: www.elsevier.com/locate/yprep

Bordetella pertussis CyaA-RTX subdomain requires calcium ions for structural stability against proteolytic degradation

Pichaya Pojanapotha [a], Niramon Thamwiriyasati [a], Busaba Powthongchin [b], Gerd Katzenmeier [a], Chanan Angsuthanasombat [a,*]

[a] *Laboratory of Molecular Biophysics and Structural Biochemistry, Bacterial Protein Toxin Research Cluster, Institute of Molecular Biosciences, Mahidol University, Salaya Campus, Nakornpathom 73170, Thailand*
[b] *Department of Biopharmacy, Faculty of Pharmacy, Silpakorn University, Nakornpathom 73000, Thailand*

ARTICLE INFO

Article history:
Received 1 July 2010
and in revised form 25 July 2010
Available online 4 August 2010

Keywords:
Adenylate cyclase-hemolysin toxin
β-Roll structure
RTX
Calcium-binding site
Proteolytic degradation

ABSTRACT

Previously, the 126-kDa *Bordetella pertussis* CyaA pore-forming (CyaA-PF) domain expressed in *Escherichia coli* was shown to retain its hemolytic activity. Here, a 100-kDa RTX (Repeat-in-ToXin) subcloned fragment (CyaA-RTX) containing a number of putative calcium-binding repeats was further investigated. The recombinant CyaA-RTX protein, although expressed as a soluble form in a protease-deficient *E. coli* strain BL21(DE3)pLysS, was found to be highly sensitive to proteolytic degradation. Interestingly, the addition of calcium ions in a millimolar range into the CyaA-RTX preparation significantly prevented the degradation. Moreover, levels of proteolytic degradation were dependent on calcium concentrations, implying an important role for calcium-binding sites in the RTX subdomain for structural stability. Homology-based modeling of the repetitive blocks in the CyaA-RTX subdomain supports that this calcium-bound protein folds into a parallel β-roll structure with calcium ions acting as a structural stabilizing bridge.

Introduction

Adenylate cyclase-hemolysin toxin (CyaA)[1] is a virulence factor secreted from *Bordetella pertussis*, a causative agent of whooping cough [1,2]. It is classified into the RTX (Repeat-in-ToXin) family due to its tandem repeated nonapeptides, Gly-Gly-X-Gly-X-Asp-X-U-X (X = any amino acid, U = large hydrophobic amino acid such as Leu, Ile, etc.), which are the putative calcium-binding sites [3]. CyaA is a 1706-residue toxin composed of two functional domains that work independently *in vitro*; an N-terminal adenylate cyclase (AC) domain (~400 residues) and a pore-forming (PF) or hemolysin (Hly) domain located ~1300 residues at the C-terminus [4]. As illustrated in Fig. 1, the pore-forming domain (CyaA-PF) contains a hydrophobic region (residues 500–700) and a calcium-binding repeat region (residues 1000–1600) comprising five blocks of the tandem Gly-Asp-rich repeats [3,5].

CyaA or CyaA-PF can be activated *via* palmitoylation at Lys^{983} by CyaC acyltransferase to be hemolytically active against sheep erythrocytes [6–8]. This fatty acylation has also been shown to increase binding affinity to the target cells and to promote delivery of the AC enzymatic domain into target cells [9,10]. It has been demonstrated that the AC domain can be internalized into $CD11b^{+}$-CHO cells and subsequently activated by calmodulin to produce pathological levels of cAMP [4,11], leading to apoptotic cell death [12]. In addition, both AC intoxication and pore formation have been revealed to be synergized for greater toxicity against target cells [10].

Thus far, αMβ2 (CD11b/CD18) integrin has been identified as a CyaA receptor in primary target cells including monocytes, macrophages, dendritic cells and neutrophils [11]. Recently, it has been shown for RTX toxins, including *B. pertussis* CyaA, *Mannheimia haemolytica* leukotoxin and *Escherichia coli* α-hemolysin (HlyA), that the oligosaccharide chains of both α- and β-subunits are required for initial interactions between the toxins and their target cells whereas the polypeptide chain of α-subunit (CD11) is responsible for specific recognition [13].

Several studies have indicated that biological activities of the RTXs require calcium ions. For instance, the calcium-binding RTX region of HlyA is responsible for the initial steps of toxin docking to the target membrane [14]. Also, autocatalytic activity of *Neisse-*

* Corresponding author. Fax: +66 662 4419906.
E-mail address: stcas@mahidol.ac.th (C. Angsuthanasombat).

[1] *Abbreviations used:* AC, adenylate cyclase; BCIP, 5-bromo-4-chloro-3-indolyl phosphate; BLAST, basic local alignment search tool; BSA, bovine serum albumin; CyaA, adenylate cyclase-hemolysin toxin; CyaA-PF, CyaA pore-forming; EDTA, ethylene diamine tetraacetic acid; EGTA, ethylene glycol tetraacetic acid; FPLC, fast-performance liquid chromatography; IPTG, isopropyl-β-D-thiogalactopyranoside; NBT, nitroblue tetrazolium; PCR, polymerase chain reaction; PMSF, phenyl methyl sulfonyl fluoride; RTX, repeat-in-toxin; SDS–PAGE, sodium dodecyl sulfate–polyacrylamide gel electrophoresis.

1046-5928/$ - see front matter © 2010 Elsevier Inc. All rights reserved.
doi:10.1016/j.pep.2010.07.012

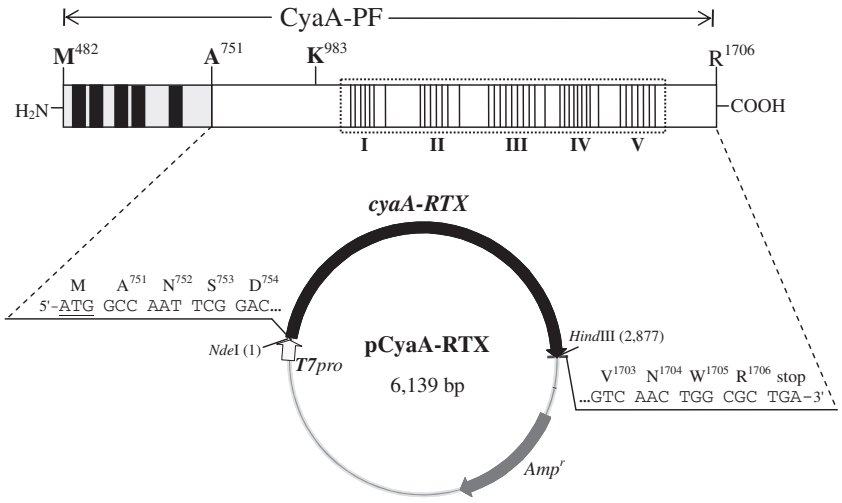

Fig. 1. Schematic map of the recombinant plasmid, pCyaA-RTX, derived from pCyaA-PF that contains the gene encoding the pore-forming domain of CyaA (CyaA-PF, residues 482–1706). The start ATG codon was underlined. The added *Nde*I restriction site was generated by PCR-based mutagenesis. T7*pro* and *Amp*^{r} symbolize the T7 promotor and ampicillin resistance gene, respectively. The black boxes represent five predicted helices that are located in the hydrophobic part (grey) and are involved in pore formation. K^{983} indicates the acylation site. The calcium-binding repeat region (highlighted with the dotted border) is organized into five repetitive blocks (I-V); block I: Gly^{1015}-Lys^{1088}, block II: Gly^{1138}-Asp^{1211}, block III: Gly^{1247}-Asp^{1353}, block IV: Gly^{1377}-Asp^{1485} and block V: Gly^{1529}-Leu^{1591}. Each line corresponds to one repeat (Gly-Gly-X-Gly-X-Asp-X-U-X).

ria meningitidis FrpC (RTX iron-regulated protein) can be induced by calcium ions at physiological concentrations [15]. In the case of CyaA, the RTX region was demonstrated to contain ~30 calcium-binding sites [3] which are shown to be essential for toxin–receptor interactions [10] and AC internalization [16,17]. Moreover, it has been demonstrated that channel formation and hemolytic activity of CyaA are dependent on calcium concentrations [18,19]. However, the structural role of calcium in the RTX members particularly for CyaA has not been delineated. In this study, we have clearly demonstrated that calcium ion is an important determinant of the structural stability against proteolytic degradation of the CyaA-RTX subdomain. In addition, homology modeling of its individual tandem-repeat blocks revealed that calcium ions are required to occupy the space in the β-roll structure, serving as a structural stabilizing link.

Materials and methods

Construction of recombinant plasmid

The pCyaA-PF plasmid encoding the hemolysin domain of CyaA [7] was used as a template for PCR-based mutagenesis following the procedure of the QuikChange Mutagenesis Kit (Stratagene, USA). A pair of mutagenic oligonucleotides (Sigma–Aldrich, Singapore) was used to generate an additional *NdeI* restriction site at base positions 2245–2250 of the *cyaA* gene; forward primer: 5′-CACGAACA**TA**TGGCCAATTCGGACG-3′ and reverse primer: 5′-GAATTGGCCA**TA**TGTTCGTGACGCG-3′ (underlined bases indicate an *NdeI* site and bold letters indicate mutated nucleotides). The PCR product was transformed into *E. coli* JM109 and then the extracted plasmid was digested by *NdeI*. The 6.1-kb *NdeI* fragment was gel-purified prior to re-ligation, giving the resultant plasmid, pCyaA-RTX, expressing the 100-kDa RTX subdomain (residues 751–1706) as shown in Fig. 1. The plasmid was re-transformed into the expression host, a protease-deficient *E. coli* strain BL21(DE3)-pLysS, and the gene segment was verified by DNA sequencing (Macrogen Inc., Korea).

Protein expression and purification

Escherichia coli BL21(DE3)pLysS cells harboring the pCyaA-RTX plasmid were grown at 37 °C, 250 rpm in Luria–Bertani broth supplemented with 100 μg/ml ampicillin. When the culture reached OD_{600} 0.4–0.5, IPTG was added to a final concentration of 0.1 mM, and incubation was continued for 3 h. Cells expressing the protein were harvested by centrifugation (6000*g*, 10 min). The pellet (~2.5 g of wet weight from 1 l of cell culture) was resuspended in 80 ml of 50 mM Tris–HCl (pH 8.0) and then disrupted in a French Pressure cell at 12,000 psi in the presence of protease inhibitors/$CaCl_2$ as indicated in the figure legends. Cell lysates were centrifuged at 13,000*g* (4 °C, 15 min) and the supernatant (after being adjusted to a total protein concentration of ~1 mg/ml; see Table 1) containing expressed proteins was verified by SDS–PAGE and Western blot analysis.

Purification was accomplished using an anion-exchange FPLC system (5 ml HiTrap Q HP, GE Healthcare Bio-sciences). The column was equilibrated with buffer A (50 mM Tris–HCl (pH 8.0), 5 mM $CaCl_2$) before injection of ~3 mg of lysate supernatant (1 mg/ml). Subsequently, the column was washed with 5% B in A (B = buffer A containing 1 M NaCl) and the CyaA-RTX fragment was eluted at 7.5% B in A at a flow rate of 0.5 ml/min. Eluted fractions containing the 100-kDa CyaA-RTX protein were pooled and the purity of samples was analyzed by SDS–PAGE. Protein concentrations were measured by Bradford microassay (Bio-RAD) using BSA fraction V (Sigma–Aldrich, USA) as a standard protein.

Western blot analysis

Protein samples analyzed by 10% SDS–PAGE were transferred to a nitrocellulose membrane which was subsequently blocked with 5% skim milk-PBS (120 mM NaCl, 16 mM Na_2HPO_4, 4 mM KH_2PO_4, pH 7.4). The blotted proteins were probed with the 9D4 anti-RTX monoclonal antibody (Listlabs, USA 1:4000 dilution). The immunocomplexes were detected with alkaline phosphatase-conjugated goat anti-mouse IgG antibody (Pierce, 1:20,000 dilution) and visualized by interacting with BCIP/NBT (Sigma).

Proteolytic susceptibility test

To observe the effect of protease inhibitors, cell lysates expressing the CyaA-RTX protein were incubated at 4 °C overnight in the presence of 100 mM EDTA; 50 mM 1,10-phenanthroline; 1 mM PMSF; 10 μg/ml pepstatin; 10 μg/ml leupeptin; 10 μg/ml aprotinin; 2 mM $MgCl_2$ or 2 mM $CaCl_2$ as indicated. Effects of calcium

Table 1
Purification of recombinant CyaA-RTX expressed in *E. coli*.

Fraction	Volume (ml)	Total protein[b] (mg)	CyaA-RTX[c] (mg)	Yield (%)	Purity[c] (%)
Cell lysate[a]	100	~100	25–35	100	25–35
HiTrapQ HP	10	~22	~20	70–80	~95

[a] From ~2.5 g of wet weight cell pellet (from 1 l of culture).
[b] Protein concentration was determined by Bradford microassay using BSA as a standard.
[c] The relative amount and the percentage purity were estimated from SDS–PAGE gels.

on the protein stability were examined by incubating the purified protein at 37 °C for different time ranges with various $CaCl_2$ concentrations. The inhibitory effect was then analyzed by SDS–PAGE.

N-terminal amino acid sequencing

Proteins separated by 10% SDS–PAGE were electroblotted onto a polyvinylidene difluoride membrane (Immobilon-P, Millipore) by using Mini Trans-Blot apparatus (Bio-Rad) and subsequently visualized by Coomassie-blue staining. Protein bands were excised and analyzed by N-terminal sequencing using an ABI-491 automated protein sequencer (Proteome Factory, Germany).

Homology-based modeling

Initially, the best-fit template structures searched from the Protein Data Bank (BLAST) were selected based on their resolution and amino acid sequence homology against individual repetitive blocks. The models of each RTX block were constructed using the SWISS-MODEL program. Calcium ions were added into the models using their corresponding template coordinates and subsequent refinement *via* energy minimization was performed by the Chimera program.

Results and discussion

High level of soluble expression of the CyaA-RTX fragment susceptible to proteolysis

Recombinant plasmid (pCyaA-RTX) that contains a 2.8-kb gene fragment encoding the RTX subdomain of CyaA (residues 751–1706) was successfully constructed (Fig. 1). Upon IPTG-induced expression *via* the T7 promoter, the 100-kDa RTX subdomain fragment (calculated molecular mass = 99,895.67 Da) was produced at high quantities (~35 mg/l of culture; see Table 1) as a soluble protein in *E. coli* strain BL21(DE3)pLysS (Fig. 2A, lane 2). However, this 100-kDa recombinant protein migrated on SDS–PAGE with a relatively larger apparent size than the 116-kDa β-galactosidase standard marker, and the reason for this anomalous migration remains unclear. Following the ATG start codon, the deduced amino acid sequence of the recombinant CyaA-RTX fragment begins from Ala^{751} to Arg^{1706} (see Fig. 1). As shown in Fig. 3 (lane 10), N-terminal sequencing of the expressed gene product confirmed that its N-terminus (Ala-Asn-Ser-Asp-Gly—) was identical to the expected terminus of the recombinant CyaA-RTX fragment.

It should be noted that the 100-kDa CyaA-RTX fragment was expressed at a level markedly higher than the 126-kDa CyaA-PF fragment (hemolysin domain) (Fig. 2A, lanes 2 and 3, respectively). Similar observation has been noted for the murine endogenous retroviral transmembrane envelope protein that deletion of the hydrophobic transmembrane domain significantly improves the expression levels [20]. Moreover, the isolated RTX subdomain was still expressed as a soluble form presumed to adopt a native-folded conformation, signifying that the hydrophobic helices do not contribute to the structural integrity of the RTX subdomain of CyaA. However, cell lysate expressing the CyaA-RTX protein showed numerous degraded bands as detected by Western blot analysis (Fig. 2A, lane 5), although in a protease-deficient *E. coli* host. To overcome this proteolytic degradation, several protease inhibitors including EDTA, 1,10-phenanthroline, PMSF, pepstatin, leupeptin and aprotinin were added into the protein preparation. Levels of degradation were significantly decreased when the incubation was carried out in the presence of either EDTA (a general metalloprotease inhibitor), 1,10-phenanthroline (a specific zinc metalloprotease inhibitor) or PMSF (a serine protease inhibitor), whereas there was no inhibitory effect with the other inhibitors used (data not shown). The result suggested that serine proteases and zinc metalloproteases might play a key role in degradation of CyaA-RTX. However, the proteolytic degradation of this protein in the lysate could not be totally inhibited by the inhibitors.

For purification, a relatively stable band of the 100-kDa CyaA-RTX protein with ~95% purity was accomplished *via* a single-step anion-exchange chromatography in the presence of 5 mM $CaCl_2$ as analyzed by SDS–PAGE (see Fig. 3, lane 10). It is also noted that 5 mM $CaCl_2$ together with certain protease inhibitors (i.e. PMSF and 1,10-phenanthroline) are required for cell lysate preparation (see below for more details). These optimized purifying conditions allowed us to obtain sufficient amounts of the purified CyaA-RTX protein (~20 mg/l of culture; see Table 1) for further investigations of its properties.

Requirement of calcium ions on structural stability of the 100-kDa CyaA-RTX protein

Since CyaA-RTX contains calcium-binding Gly-Asp-rich repeats [17], we therefore hypothesized that binding to calcium ions would promote a stably folded conformation in the CyaA-RTX subdomain. To test this hypothesis, $CaCl_2$ was added into the protein preparation and titrated in a hundred-fold serial dilution. As demonstrated in Fig. 2B, the result showed that 2 mM $CaCl_2$ (lane 5), but not $MgCl_2$, (lane 6) was able to reduce proteolytic degradation of the CyaA-RTX protein, indicating that its stably folded structure could be specifically enhanced by calcium ions. Moreover, excess quantity of EDTA (at 100 mM) was found to be less efficient in reduction of protein degradation (Fig. 2B, lane 7), suggesting that the binding with calcium of CyaA-RTX plays more important role in preventing protein degradation than the removal of a metal ion protease cofactor. It has been recently shown by circular dichroism analysis that the CyaA-RTX fragment (residues 1006–1706) was highly unstructured in the absence of calcium ions, but became more structured when in the presence of 2 mM $CaCl_2$ [21]. Altogether, these data suggest that a calcium-induced conformational transformation is necessary for the structural stability of the CyaA-RTX molecule, and hence less susceptible to proteolytic attack.

Further attempts were made to investigate the effect of calcium concentrations on the RTX stability for an extended time of incubation. Degradation profiles observed when the purified RTX samples were incubated at 37 °C for 1, 3 or 7 days revealed that the stability of the 100-kDa RTX band notably increases as supplemented with

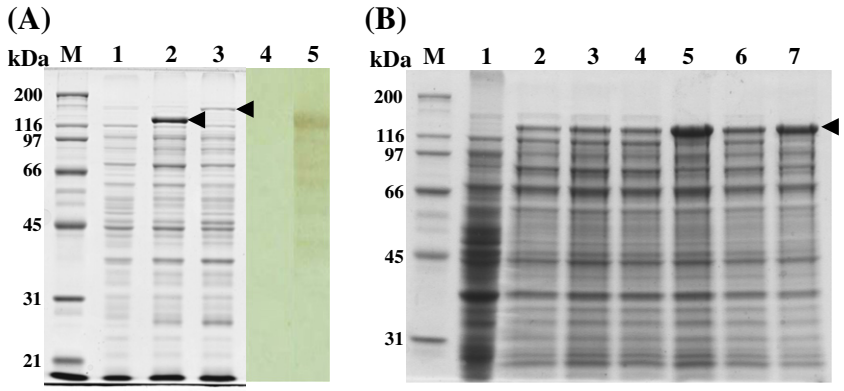

Fig. 2. SDS–PAGE analysis (Coomassie brilliant blue-stained 10% gel) of (A) crude extracts of *E. coli* cells containing the pET-17b vector (lane 1), or expressing either the 100-kDa CyaA-RTX protein (lane 2) or the 126-kDa CyaA-PF protein (lane 3). Lanes 4 and 5 are Western blot analysis of their corresponding lysates of lanes 1and 2, respectively. (B) Crude cell lysates expressing the CyaA-RTX protein were kept overnight at 4 °C without additives (lane 2), or supplemented with 0.2 μM, 20 μM and 2 mM $CaCl_2$ (lanes 3, 4 and 5 respectively), or with 2 mM $MgCl_2$ (lane 6) or 100 mM EDTA (lane 7). Lane 1 is *E. coli* cells harboring pET-17b vector. Lane M represents the molecular mass standards. Arrow indicates the band corresponding to the 100-kDa CyaA-RTX protein.

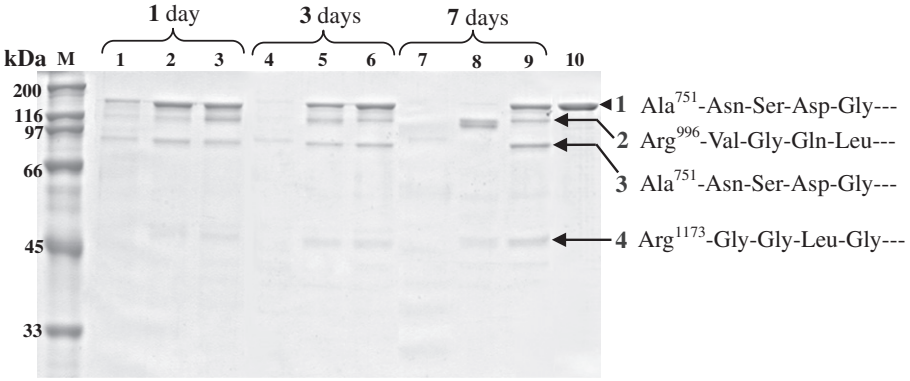

Fig. 3. SDS–PAGE analysis (Coomassie brilliant blue-stained 10% gel) of the 100-kDa purified CyaA-RTX protein in 50 mM Tris–HCl (pH 8.0) buffer containing 5 mM $CaCl_2$ (lanes 1–10). The protein samples were incubated at 37 °C for 1, 3 and 7 days in the presence of 10 mM EGTA (lanes 1, 4 and 7, respectively), 3 mM EGTA (lanes 2, 5 and 8, respectively) or in the absence of EGTA (lanes 3, 6 and 9, respectively). Lane 10 represents the purified sample without incubation at 37 °C. Corresponding N-terminal amino acid sequences of four major protease-resistant fragments are shown.

$CaCl_2$ at 5 mM rather than at 2 mM (Fig. 3, lanes 8 and 9). This may be suggestive of dissimilar induced-folded RTX conformations formed at these two different calcium concentrations. Nevertheless, degradation patterns of CyaA-RTX are relatively the same when compared between 5 and 10 mM $CaCl_2$ (data not shown), possibly indicating that there is no additional conformational change occurring for the supplementation of $CaCl_2$ exceeding 5 mM. On the other hand, adding a Ca^{2+}-chelating agent (i.e. EGTA) has an adverse effect on protein stability of CyaA-RTX (see Fig 3, lanes 1, 2, 4, 5, 7 and 8), signifying a reversible binding of Ca^{2+} ions to the RTX protein for their structural role. It is also noteworthy that the specific proteolytic pattern was observed herein (three major protease-resistant fragments as verified by N-terminal sequencing, see Fig. 3, lane 9).

Homology-based RTX repetitive models with structural implications for calcium ions

As mentioned earlier, the repetitive sequence in CyaA could be divided into five blocks according to the Gly-Asp-rich repeats: block $I_{1015–1088}$, block $II_{1138–1211}$, block $III_{1247–1353}$, block $IV_{1377-1485}$ and block $V_{1529–1591}$ (see Fig. 1). Since the crystal structure of CyaA has not been thus far resolved, a plausible 3D structure of each repetitive block was constructed by template-based modeling. Their best-fit template known structures include *Erwinia chrysanthemi* protease C [22] for block I (with 61.0% sequence homology), *Pseudomonas* psychrophilic alkaline protease [23] for blocks II and V (with 59.6% and 63.0% homology, respectively) and *P. aeruginosa* alkaline protease [24] for blocks III and IV (with 66.7% and 57.1% homology, respectively) (Fig. 4, left panel). The evaluated stereochemical quality revealed overall G-factor values in the satisfactory range, i.e. −0.06, −0.07, 0.01, −0.15 and −0.08 for the models of blocks I, II, III, IV and V, respectively. In addition, the Ramachandran plots of φ/ψ backbone-dihedral angles for all five models revealed that over 90% of the non-glycine and non-proline residues are found in the energetically preferred regions (plots not shown), indicating that the backbone stereochemistry is correlated with their corresponding side-chain conformations.

As can be inferred from all the five models (Fig. 4, right panel), calcium ions are located in the middle of two Gly-Gly-X-Gly-X-Asp loops, and there are at least three potential calcium-binding sites in each modeled block. In addition, side-chains of the 6th residues (i.e. Asp) of the repetitive loops, which provide a relative charge for calcium coordination, are well-organized into the same ion-bearing structure. Thus, calcium ions can fit properly into the space between the loops for serving as a bridge to hold the parallel beta rolls together (see Fig. 4, inset for block V). Nevertheless, further specific mutagenesis of these proposed calcium-coordinating residues is needed to elucidate their contribution to the structural stability.

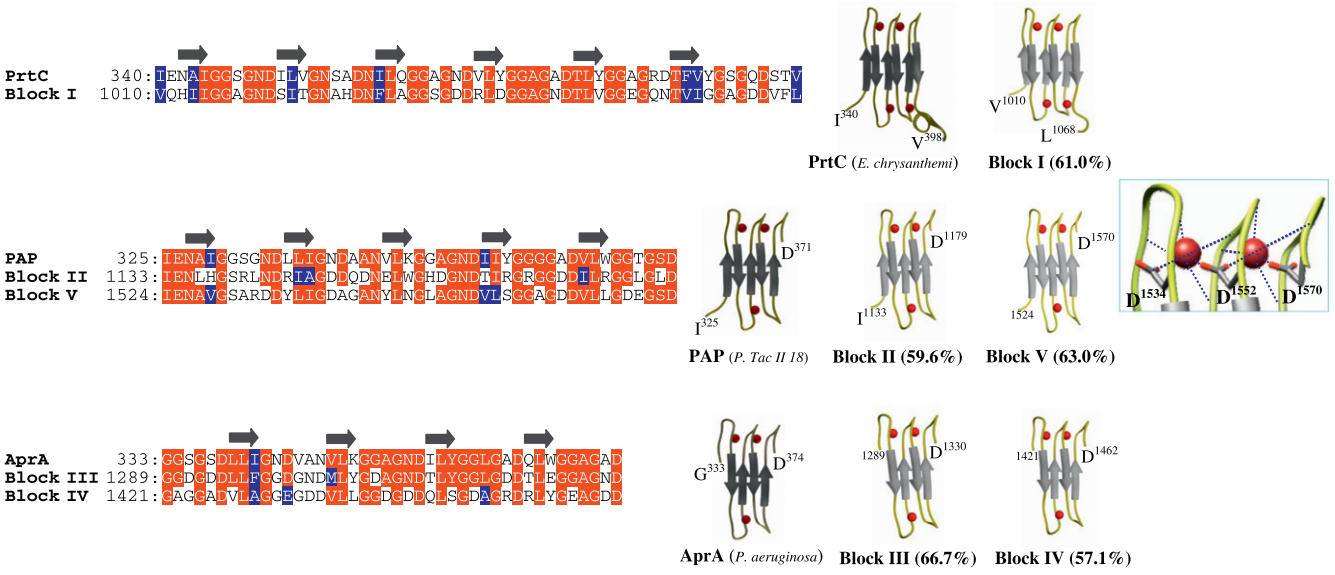

Fig. 4. (Left panel) Alignments of amino acid sequence from individual CyaA-RTX repetitive blocks (I-V) with their most matching templates of known structures; block I (Val^{1010}-Leu^{1068}) with PrtC (protease C from *Erwinia chrysanthemi*, PDB code: 1k7g), blocks II (Ile^{1133}-Asp^{1179}) and V (Ile^{1524}- Asp^{1570}) with PAP (psychrophilic alkaline protease from *Pseudomonas* Tac II 18, PDB code: 1g9k), blocks III (Gly^{1289}-Asp^{1330}) and IV (Gly^{1421}-Asp^{1462}) with AprA (alkaline protease from *Pseudomonas aeruginosa*, PDB code: 1kap). The positions of β-strands of template structures are illustrated over the alignments. Red and blue shadings indicate sequence identity and homology, respectively. (Right panel) Ribbon diagrams of the three crystal structure templates (black) and their derived homology models (grey) of each repetitive block. Red balls represent calcium ions bound to the proteins. The percentages of sequence homology are shown in parentheses. Inset, the zoomed region of block V that illustrates two calcium ions bound between the repetitive loops by the 6th Asp residues (i.e. Asp^{1534}, Asp^{1552} and Asp^{1570}) and backbone carbonyls.

In conclusion, we have here provided pivotal evidence for the first time that the 100-kDa CyaA-RTX subdomain, over-expressed separately as a soluble protein, absolutely requires calcium ions in a millimolar range for its structural stability against proteolytic degradation. 3D models of each repetitive block can show that their parallel β-roll structures have need of calcium ions to be a structural stabilizing link. However, it remains a challenge for determining the crystal structure of either CyaA-RTX or CyaA-PF that would provide more structural and functional details of their mechanistic basis of action.

Acknowledgments

This work was funded in part by the Commission of Higher Education. PhD scholarship from the Medical Scholars Program, Mahidol University (to P.P.) and Royal Golden Jubilee PhD scholarship (to N.T.) and postdoctoral fellowship (to B.P.) from the Thailand Research Fund are gratefully acknowledged.

References

[1] N.H. Carbonetti, G.V. Artamonava, C. Andreasen, N. Bushar, Pertussis toxin and adenylate cyclase toxin provide a one-two punch for establishment of *Bordetella pertussis* infection of the respiratory tract, Infect. Immun. 73 (2005) 2698–2703.
[2] S.R. Paccani, F.D. Molin, M. Benagiano, D. Ladant, M.M. D'Elios, C. Montecucco, C.T. Baldari, Suppression of T-lymphocyte activation and chemotaxis by the adenylate cyclase toxin of *Bordetella pertussis*, Infect. Immun. 76 (2008) 2822–2832.
[3] C. Bauche, A. Chenal, O. Knapp, C. Bodenreider, R. Benz, A. Chaffotte, D. Ladant, Structural and functional characterization of an essential RTX subdomain of *Bordetella pertussis* adenylate cyclase toxin, J. Biol. Chem. 281 (2006) 16914–16926.
[4] Q. Guo, Y. Shen, Y.S. Lee, C.S. Gibbs, M. Mrksich, W.J. Tang, Structural basis for the interaction of *Bordetella pertussis* adenylyl cyclase toxin with calmodulin, EMBO J. 24 (2005) 3190–3201.
[5] J. Vojtova, J. Kamanova, P. Sebo, *Bordetella* adenylate cyclase toxin: a swift saboteur of host defense, Curr. Opin. Microbiol. 9 (2005) 1–7.
[6] M. Hackett, L. Guo, J. Shabanowitz, D.F. Hunt, E.L. Hewlett, Internal lysine palmitoylation in adenylate cyclase toxin from *Bordetella pertussis*, Science 266 (1994) 433–435.
[7] B. Powthongchin, C. Angsuthanasombat, High level of soluble expression in *Escherichia coli* and characterisation of the CyaA pore-forming fragment from a *Bordetella pertussis* Thai clinical isolate, Arch. Microbiol. 189 (2008) 169–174.
[8] N. Thamwiriyasati, B. Powthongchin, J. Kittiworakarn, G. Katzenmeier, C. Angsuthanasombat, Esterase activity of *Bordetella pertussis* CyaC-acyltransferase against synthetic substrates: implications for catalytic mechanism in vivo, FEMS Microbiol. Lett. 340 (2010) 183–190.
[9] M. El-Azami-El-Idrissi, C. Bauche, J. Loucka, R. Osicka, P. Sebo, D. Ladant, C. Leclerc, Interaction of *Bordetella pertussis* adenylate cyclase with CD11b/CD18: role of toxin acylation and identification of the main integrin interaction domain, J. Biol. Chem. 278 (2003) 38514–38521.
[10] E.L. Hewlett, G.M. Donato, M.C. Gray, Macrophage cytotoxicity produced by adenylate cyclase toxin from *Bordetella pertussis*: more than just making cyclic AMP!, Mol. Microbiol. 59 (2006) 447–459.
[11] P. Guermonprez, N. Khelef, E. Blouin, P. Rieu, P.R. Castagnoli, N. Guiso, D. Ladant, C. Leclerc, The adenylate cyclase toxin of *Bordetella pertussis* binds to target cells via the αMβ2 integrin (CD11b/CD18), J. Exp. Med. 193 (2001) 1035–1044.
[12] N. Khelef, A. Zychlinsky, N. Guiso, *Bordetella pertussis* induces apoptosis in macrophages: role of adenylate cyclase hemolysin, Infect. Immun. 61 (1993) 4064–4071.
[13] J. Morova, R. Osicka, J. Masin, P. Sebo, RTX cytotoxins recognize 2 integrin receptors through N-linked oligosaccharides, Proc. Natl. Acad. Sci. USA 105 (2008) 5355–5360.
[14] L.S. Magraner, A.R. Viguera, M.G. Pacios, M.P. Garcillan, J.R. Arrondo, F. Cruz, F.M. Goni, H. Ostolaza, The calcium-binding C-terminal domain of *Escherichia coli* hemolysin is a major determinant in the surface-active properties of the protein, J. Biol. Chem. 282 (2007) 11827–11835.
[15] R. Osicka, K. Prochazkova, M. Sulc, I. Linhartova, V. Havlicek, P. Sebo, A novel "clip-and-link" activity of repeat in toxin (RTX) proteins from gram-negative pathogens: covalent protein cross-linking by an Asp-Lys isopeptide bond upon calcium-dependent processing at an Asp-Pro bond, J. Biol. Chem. 279 (2004) 24944–24956.
[16] F. Gentile, A. Raptis, L.G. Knipling, J. Wolff, *Bordetella pertussis* adenylate cyclase penetration into host cells, Eur. J. Biochem. 175 (1988) 447–453.
[17] T. Rose, P. Sebo, J. Bellalou, D. Ladant, Interaction of calcium with *Bordetella pertussis* adenylate cyclase toxin: characterization of multiple calcium-binding sites and calcium-induced conformational changes, J. Biol. Chem. 270 (1995) 26370–26376.
[18] I.E. Ehrmann, M.C. Gray, V.M. Gordon, L.S. Gray, E.L. Hewlett, Hemolytic activity of adenylate cyclase toxin from *Bordetella pertussis*, FEBS Lett. 278 (1991) 79–83.
[19] O. Knapp, E. Maier, G. Polleichtner, J. Masin, P. Sebo, R. Benz, Channel formation in model membranes by the adenylate cyclase toxin of *Bordetella pertussis*: effect of calcium, Biochem. J. 42 (2003) 8077–8084.
[20] K.S. Kim, K.H. Kim, S.E. Choi, J.W. Yoon, Y. Kang, Soluble expression in *Escherichia coli* of murine endogenous retroviral transmembrane envelope

protein having immunosuppressive activity, Prot. Expres. Purif. 16 (1999) 19–26.
[21] A. Chenal, J.I. Guijarro, B. Raynal, M. Delepierre, D. Ladant, RTX calcium binding motifs are intrinsically disordered in the absence of calcium: implication for protein secretion, J. Biol. Chem. 284 (2009) 1781–1789.
[22] T. Hege, U. Baumann, Protease C of *Erwinia chrysanthemi*: the crystal structure and role of amino acids Y228 and E189, J. Mol. Biol. 314 (2001) 187–193.
[23] N. Aghajari, F.V. Petegem, V. Villeret, J.P. Chessa, C. Gerday, R. Haser, J.V. Beeumen, Crystal structures of a psychrophilic metalloprotease reveal new insights into catalysis by cold-adapted proteases, Proteins 50 (2003) 636–647.
[24] U. Baumann, S. Wu, K.M. Flaherty, D.B. McKay, Three-dimensional structure of the alkaline protease of *Pseudomonas aeruginosa*: a two-domain protein with a calcium binding parallel beta roll motif, EMBO J. 12 (1993) 3357–3364.